Bol. Soc. Paran. Mat.
©SPM – E-ISSN-2175-1188
SPM: www.spm.uem.br/bspm

(3s.) **v. 2026 (44) 7** : 1–13.
ISSN-0037-8712
doi:10.5269/bspm.81707

Solution of Some Problem of Heat and Mass Transfer on the Peristaltic Flow in Symmetric Channel with Sinusoidal Walls

Hanan S. Gafel, Luluah G. Albugami, S. H. Elhag and Mushrifah A. S. Al-Malki

ABSTRACT: This study investigates the influence of heat transfer, mass transfer, and magnetic fields on the peristaltic motion of a Rabinowitsch-type fluid within an inclined conduit. Thermal and concentration transport phenomena under magnetic effects are modeled by considering an incompressible Rabinowitsch fluid in an inclined channel. The governing equations are simplified through the long-wavelength approximation and the assumption of a low Reynolds number, and are subsequently solved analytically using MATHEMATICA with appropriate boundary conditions. The analysis addresses several flow characteristics, including temperature distribution, velocity profiles, tangential stress, pressure variations, net pressure difference, and frictional resistance. Numerical simulations are employed to evaluate these parameters, and the combined impacts of magnetic fields, heat transfer, and mass transfer on peristaltic transport are systematically examined. Graphical results are presented to illustrate the findings. The outcomes of this research are especially relevant to biomedical applications, particularly in modeling the propulsion of digestive fluids in the intestines during endoscopic procedures.

Key Words: Magnetic field, mass transfer, heat transfer peristaltic flow, an inclined conduit, Rabinowitsch fluid model.

Contents

1. Introduction

Due to its broad applications in both physiological and industrial fields, the peristaltic mechanism has received substantial attention from researchers in recent years. This flow process is evident in numerous biological systems, exemplified by food being pushed through the esophagus, urine flow moving from the kidneys toward the bladder, and reproductive functions. Gafel [17] conducted a study analyzing the influence of magnetic fields, heat, and mass transfer on peristaltic motion in a porous channel using a mathematical model focused on velocity and thermal behavior. Gafel [15] also performed a study exploring how a magnetic field affects the peristaltic motion of a fractional Maxwell fluid within a tube, particularly focusing on heat transfer aspects. The research utilized the fractional Maxwell framework, incorporating assumptions of a low Reynolds number and long-wavelength approximation. Both analytical and numerical methods were applied, enhancing insight into biomechanical and engineering systems. In a separate investigation, Gafel [16] examined heat transfer in peristaltic blood flow through an inclined asymmetric channel influenced by a tilted magnetic field. The study evaluated Hartmann number effects on velocity and noted an inverse link between frictional force and pressure increase. Particle-laden fluids are extensively applied in industrial, chemical, and biological systems. Saffman [33] was among the earliest researchers to investigate and formulate models for the two-phase flow issue in this context. The

2020 *Mathematics Subject Classification:* 76A05, 76Z05, 80A20
Submitted February 02, 2026. Published April 11, 2026

movement of dust-laden fluids through peristaltic action, examined under the long-wavelength approximation conditions was analyzed by Srinivasacharya et al. [37] Additionally, Zeeshan et al. [46] conducted numerical simulations on the peristaltic behavior of dusty nanofluids in a curved channel. The study of fluid movement through permeable biological channels is crucial in contexts such as the bile duct, respiratory passages, gallbladder affected by stones, and small blood vessels. In this regard, Elshehawey et al. [14] analyzed fluid flow in a porous asymmetric channel using the assumptions of long-wavelength and low Reynolds number. In a related contribution, Khan and Tariq [23] investigated the peristaltic transport of a second-grade dusty fluid in a porous asymmetric channel while considering slip boundary conditions. Parthasarathy et al. [29] explored magnetohydrodynamic (MHD) dusty fluid with peristaltic motion in porous media. Additional recent contributions include works by other researchers [6, 11, 12]. Due to its application in designing various industrial and mechanical systems, heat transfer in dusty fluid flows within channels has gained research prominence. This process is also significant in fields such as petroleum extraction, fluidized systems, crude oil refining, polymer engineering, fluid sprays, and gas cooling. It holds vital importance in medical procedures like hemodialysis and blood oxygenation. The investigation of heat transfer in dusty fluids within channels has drawn considerable interest due to its extensive industrial and engineering relevance. This behavior is evident in sectors such as oil and gas production, fluidization systems, crude oil processing, polymer manufacturing, droplet spray technologies, and gas cooling mechanisms. Given its vital role in medical treatments like hemodialysis and oxygen exchange, the impact of heat transfer on peristaltic fluid transport has increasingly attracted research attention. Lakshminarayana et al. [25] examined the role of heat and slip conditions on the peristaltic motion of an electrically conducting Bingham fluid under low Reynolds number and long wavelength. Iqbal et al. [21] investigated Sisko fluid peristalsis in an asymmetric geometry. Makinde and Gnaneswara [26] examined heat transfer phenomena associated with the peristaltic flow of Casson fluid in an asymmetric, permeable channel. Ramesh and Devakar [31] investigated the influence of heat transfer on the peristaltic motion of magnetohydrodynamic (MHD) second-grade fluids through porous asymmetric channels. In another study, Hayat et al. [19] highlighted the impact of thermal radiation on the peristaltic transport of dusty fluids. Kalpana and Saleem [22] investigated the thermal behavior of dusty fluid within an irregularly inclined channel subjected to an inclined magnetic field. Varjravelu et al. [45] analyzed the peristaltic transport of Jeffrey fluid with heat transfer effects, employing the assumptions of long-wavelength and low Reynolds number. Additionally, Selvi et al. [34] studied fluid motion in a vertical porous duct. The influence of heat transfer on the peristaltic transport of Jeffrey fluid through inclined porous layers has been examined. Hafez et al. [18] studied second-grade fluid motion in a tube while accounting for thermal effects. Zhang et al. [47] carried out a thermal investigation of sinusoidal particle–fluid interaction under the assumptions of long-wavelength and low Reynolds number. Iqbal et al. [20] explored the peristaltic behavior of Maxwell fluid in a symmetric channel, incorporating both mass and heat convection. Furthermore, Chandrawat et al. [9] investigated heat transfer effects on the unsteady motion of immiscible dusty and clear fluids. Several related studies have examined the peristaltic flow of both Newtonian and non-Newtonian fluids in recent years [27, 28, 32, 36]. Notable research in this area includes works on the flow of these fluids, as seen in references [7, 10, 24, 30, 35, 38-44]. Recent advancements in the understanding of heat and mass transfer phenomena have been discussed in [1-4]. This study investigates the impact of heat and mass transfer on the magnetohydrodynamic (MHD) flow of Rabinowitsch fluid in a peristaltic context. A comprehensive understanding of peristalsis involves a deep knowledge of the Rabinowitsch fluid model, especially focusing on how viscosity influences the fluid's behavior. The present study investigates the influence of heat transfer, mass transport, and magnetic field on the peristaltic motion of a Rabinowitsch fluid with variable viscosity in a two-dimensional symmetric channel. The analysis is carried out under the assumptions of long-wavelength and low Reynolds number. Analytical expressions are obtained for temperature, velocity, tangential stress, and other relevant flow parameters. The frictional force, pressure rise, and gradient were also analyzed. The effects of several novel parameters were then examined using these solutions, and the findings were thoroughly discussed and graphically represented. Keeping all above mentioned studies in mind, we can say that no single study is available on the peristaltic flow of Rabinowitsch fluid flow through inclined channel with heat and mass transfer simultaneously. Moreover, the effects of convective heat and mass transfer at the boundaries under such consideration is studied before. Under the impact of the magnetic field, mass transfer studies are conducted. Moreover, thechannel inclination is included in the analysis. By using a lubrication method, the resulting equations are first modelled and then made simpler. By using MATHEMATICA to calculate exact answers, results are illustrated graphically. Main purpose behind performing this study is to develop a mathematical model which can be applied to study peristaltic flow within human body as convective heat and mass transfer are main processes involved. This study aims to explore the effects of an inclined magnetic field, heat and mass transfer, and the yield stress characteristics of Rabinowitsch fluid on peristaltic flow in an inclined channel, focusing on pure convection. The main objective is to develop a mathematical model for investigating convective heat transfer during peristaltic motion of Rabinowitsch fluid, particularly in the human body. Applications of this research include modeling peristaltic transport and flow dynamics in an inclined channel. Additionally, the study contributes to understanding how peristaltic flow influences drug delivery efficiency within the human body using the Rabinowitsch fluid model. Chemical engineers can apply these findings to improve flow transport and mixing processes.

2. Flow Description

The current analysis is performed to study the 2-dimensional peristaltic flow of Rabinowitsch fluid in an inclined channel with heat and mass transfer. In addition, we also analyze the impact of magnetic field, heat and mass transfer effect on the flow. For problem under consideration, geometry is exhibited in Cartesian coordinates system . Furthermore, the fluid flow is caused by the meta chronal wave, resulting from uniform cilia beating whereas the temperature and concentration at the wall are and respectively (see Fig. 1).

2.1. The problem's mathematical formulation

This study considers a model of peristaltic transport for an incompressible Rabinowitsch fluid within a uniformly inclined channel, as illustrated in Fig. 1. The configuration consists of a two-dimensional symmetric channel of width 2a, filled with the non-Newtonian Rabinowitsch fluid. The channel walls propagate sinusoidal waves of wavelength λ and a uniform propagation speed c; b stands for wave amplitude and t for wave duration. Below is a definition of the mathematical expression for wall surface geometry[5]:

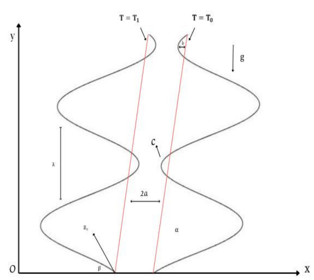

Figure 1: Geometric description of the model

$$\bar{Y} = \bar{H}(\bar{X}, \bar{t}) = a + b \sin\left(\frac{2\pi}{\lambda}(\bar{X} - c\bar{t})\right), \tag{2.1}$$

The governing equations for the flow are:

$$\frac{\partial \overline{U}}{\partial \overline{X}} + \frac{\partial \overline{V}}{\partial \overline{Y}} = 0, \tag{2.2}$$

$$\rho\left[\frac{\partial\bar{U}}{\partial\bar{t}}+\bar{U}\frac{\partial\bar{U}}{\partial\bar{X}}+\bar{V}\frac{\partial\bar{U}}{\partial\bar{Y}}\right]=-\frac{\partial\bar{P}}{\partial\bar{X}}+\frac{\partial\bar{S}_{\overline{XX}}}{\partial\bar{X}}+\frac{\partial\bar{S}_{\overline{XY}}}{\partial\bar{Y}} +\rho g\sin\alpha+\rho g\beta_1(\bar{T}-T_0) -\sigma B_0^2\cos\beta(\bar{U}\cos\beta-\bar{V}\sin\beta)+\rho g\alpha_C(\bar{C}-C_0), \tag{2.3}$$

$$\rho\left[\frac{\partial\bar{V}}{\partial\bar{t}}+\bar{U}\frac{\partial\bar{V}}{\partial\bar{X}}+\bar{V}\frac{\partial\bar{V}}{\partial\bar{Y}}\right]=-\frac{\partial\bar{P}}{\partial\bar{Y}}+\frac{\partial\bar{S}_{\overline{YX}}}{\partial\bar{X}}+\frac{\partial\bar{S}_{\overline{YY}}}{\partial\bar{Y}}-\rho g\cos\alpha-\sigma B_0^2\cos\beta\left(\bar{U}\cos\beta-\bar{V}\sin\beta\right), \tag{2.4}$$

The heat conduction equation is as follows:

$$\rho C_P\left[\frac{\partial\overline{T}}{\partial\bar{t}}+\overline{U}\frac{\partial\overline{T}}{\partial\overline{X}}+\overline{V}\frac{\partial\overline{T}}{\partial\overline{Y}}\right]=K\left(\frac{\partial^2\overline{T}}{\partial\overline{X}^2}+\frac{\partial^2\overline{T}}{\partial\overline{Y}^2}\right)+\overline{S}_{XX}\frac{\partial\overline{U}}{\partial\overline{X}}+Q_0\left(\overline{T}-T_0\right), \tag{2.5}$$

$$\left[\frac{\partial\bar{c}}{\partial\bar{t}}+\bar{U}\frac{\partial\bar{c}}{\partial\bar{X}}+\bar{V}\frac{\partial\bar{c}}{\partial\bar{Y}}\right]=D_m\left[\frac{\partial^2\bar{c}}{\partial\bar{X}^2}+\frac{\partial^2\bar{c}}{\partial\bar{Y}^2}\right]+\frac{D_mK_T}{T_m}\left[\frac{\partial^2\bar{T}}{\partial\bar{X}^2}+\frac{\partial^2\bar{T}}{\partial\bar{Y}^2}\right], \tag{2.6}$$

In the laboratory frame $(\bar{X},\bar{Y})$, the flow is unsteady. However, when observed from a moving frame traveling at the wave speed c (wave frame) $(\bar{x},\bar{y})$, it becomes steady. The two frames between velocities and coordinates are

$$\bar{x}=\bar{X}-c\bar{t},\quad \bar{y}=\bar{Y},\quad \bar{u}=\bar{U}-c\bar{t},\quad \bar{v}=\bar{V},\quad \bar{p}=\bar{P},\quad \bar{c}=c,\quad \overline{T}=T \tag{2.7}$$

The velocity components in the wave frame $(\overline{x},\overline{y})$ are denoted by $\overline{u}$ and $\overline{v}$, while the pressure in this frame is represented by $\overline{p}$. The symbol $\overline{P}$ refers to the stationary (fixed) reference frame.

The flow analysis involved introducing the following dimensionless parameters and variables.

$$\begin{aligned}
&x=\frac{\bar{x}}{\lambda},\quad y=\frac{\bar{y}}{a},\quad t=\frac{c\bar{t}}{\lambda},\quad p=\frac{a^2\bar{p}}{c\mu\lambda},\\
&\delta=\frac{a}{\lambda},\quad u=\frac{\bar{u}}{c},\quad v=\frac{\bar{v}}{c\delta},\quad Re=\frac{\rho ca}{\mu},\\
&\delta_{ij}=\frac{a\bar{\delta}_{ij}}{c\mu},\quad \theta=\frac{\overline{T}-T_0}{T_0},\quad \eta=\frac{Q_0a^2}{K},\\
&B_r=\frac{c^2\mu}{KT_0},\quad B_i=\frac{ah}{K},\quad M=B_0a\sqrt{\frac{\sigma}{\mu}},\quad \varphi=\frac{\bar{c}-c_0}{c_0}
\end{aligned} \tag{2.8}$$

Were

$$\begin{aligned}
\bar{S}_{\overline{XX}}&=\frac{2\mu}{1+\lambda_1}\left[1+\lambda_2\left(\bar{U}\frac{\partial}{\partial\bar{X}}+\bar{V}\frac{\partial}{\partial\bar{Y}}\right)\right]\frac{\partial\bar{U}}{\partial\bar{X}},\\
\bar{S}_{\overline{XY}}&=\frac{\mu}{1+\lambda_1}\left[1+\lambda_2\left(\bar{U}\frac{\partial}{\partial\bar{X}}+\bar{V}\frac{\partial}{\partial\bar{Y}}\right)\right]\left(\frac{\partial\bar{U}}{\partial\bar{Y}}+\frac{\partial\bar{V}}{\partial\bar{X}}\right),\\
\bar{S}_{\overline{YY}}&=\frac{2\mu}{1+\lambda_1}\left[1+\lambda_2\left(\bar{U}\frac{\partial}{\partial\bar{X}}+\bar{V}\frac{\partial}{\partial\bar{Y}}\right)\right]\frac{\partial\bar{V}}{\partial\bar{Y}},
\end{aligned} \tag{2.9}$$

2.2. The solution to the problem

Based on the transformations in equation (2.7) and the dimensionless variables in equation (2.8), the main governing equations (2.2)–(2.6) are simplified as follows:

$$\left(\frac{\partial u}{\partial x}+\frac{\partial v}{\partial y}\right)=0, \tag{2.10}$$

$$\operatorname{Re}\delta\left[u\frac{\partial u}{\partial x}+v\frac{\partial u}{\partial y}\right]=-\frac{\partial p}{\partial x}+c_{11}\frac{\partial^2 u}{\partial y^2}+c_{22}\sin\alpha+c_3\theta+c_4\varphi-M^2\cos\beta\left(u\cos\beta-v\sin\beta\right), \tag{2.11}$$

$$\operatorname{Re}\delta^3[\,u\frac{\partial v}{\partial x}+v\frac{\partial v}{\partial y}\,]=-\frac{\partial p}{\partial y}+\frac{\delta^2}{1+\lambda_1}\frac{\partial^2 u}{\partial x\partial y}-\delta c_{22}\cos\alpha-\delta M^2\cos\beta(u\cos\beta-v\delta\sin\beta), \tag{2.12}$$

$$\operatorname{Re}\delta\frac{aT_0C_p}{c^2}[\,u\frac{\partial\theta}{\partial x}+v\delta\frac{\partial\theta}{\partial y}\,]=\frac{1}{B_r}[\,\delta^2\frac{\partial^2\theta}{\partial x^2}+\frac{\partial^2\theta}{\partial y^2}\,]+\frac{\eta}{B_r}\theta, \tag{2.13}$$

$$c\,\delta[\,u\frac{\partial\varphi}{\partial x}+v\frac{\partial\varphi}{\partial y}\,]=\frac{D_m}{a}[\,\delta^2\frac{\partial^2\varphi}{\partial x^2}+\frac{\partial^2\varphi}{\partial y^2}\,]+\frac{D_mK_T}{T_m}\frac{T_0}{ac_0}[\,\delta^2\frac{\partial^2\theta}{\partial x^2}+\frac{\partial^2\theta}{\partial y^2}\,], \tag{2.14}$$

Were

$$\begin{aligned}
S_{xx}&=\frac{2\delta}{1+\lambda_1}\left[1+\frac{\lambda_2\delta c}{a}\left(u\frac{\partial}{\partial x}+v\frac{\partial}{\partial y}\right)\right]\frac{\partial u}{\partial x},\\
S_{xy}&=\frac{1}{1+\lambda_1}\left[1+\frac{\lambda_2\delta c}{a}\left(u\frac{\partial}{\partial x}+v\frac{\partial}{\partial y}\right)\right]\left(\frac{\partial u}{\partial y}+\delta^2\frac{\partial v}{\partial x}\right),\\
S_{yy}&=\frac{2\delta}{1+\lambda_1}\left[1+\frac{\lambda_2\delta c}{a}\left(u\frac{\partial}{\partial x}+v\frac{\partial}{\partial y}\right)\right]\frac{\partial v}{\partial y},
\end{aligned} \tag{2.15}$$

By applying the long-wavelength approximation and assuming a low Reynolds number, equations (2.10)–(2.14) are simplified and can be written in the following form:

$$-\frac{\partial p}{\partial x}+c_{11}\frac{\partial^2 u}{\partial y^2}+c_{22}\sin\alpha+c_3\theta+c_4\varphi-M^2u\cos^2\beta=0, \tag{2.16}$$

$$\frac{\partial p}{\partial y}=0, \tag{2.17}$$

$$\frac{\partial^2\theta}{\partial y^2}+\eta\theta=0, \tag{2.18}$$

$$\frac{\partial^2\varphi}{\partial y^2}+\frac{K_T}{T_m}\frac{T_0}{c_0}\frac{\partial^2\theta}{\partial y^2}=0, \tag{2.19}$$

The corresponding boundary conditions in dimensionless form are given as follows:
At the lower boundary ($y=0$), the velocity, temperature, and concentration vanish.
At the upper boundary ($y=h$), the variables are prescribed as follows:

$$u=-1,\quad \theta=\varphi=1, \tag{2.20}$$

where the upper wall position is described by the relation

$$h=1+\varepsilon\sin(2\pi x).$$

The solutions of equations (2.16)–(2.19), subject to the boundary conditions (2.20), can be written in the following form:

$$u=\left(-1-(A(B+C+D)\,e^{hM\frac{\cos\beta}{\sqrt{c_{11}}}}\right))e^{-\,yM\frac{\cos\beta}{\sqrt{c_{11}}}}+A(B+C+D), \tag{2.21}$$

$$\theta=\csc\left(h\sqrt{\eta}\right)\sin\left(y\sqrt{\eta}\right), \tag{2.22}$$

$$\varphi = \left[\frac{1}{h} + \frac{m_{11}}{h\eta}\sin(h\sqrt{\eta})\right] y - \frac{m_{11}}{\eta}\sin\left(y\sqrt{\eta}\right), \tag{2.23}$$

$$\begin{aligned}\frac{\partial p}{\partial x} &= c_{11}\frac{d^2u}{dy^2} + c_{22}\sin\alpha + c_3\left(\frac{\sin(y\sqrt{\eta})}{\sin(h\sqrt{\eta})}\right)\\ &+ c_4\left(\frac{1}{h} + \frac{m_{11}y\sin(h\sqrt{\eta})}{h\eta} - \frac{m_{11}}{\eta}\sin(y\sqrt{\eta})\right) - M^2u(y)\cos^2\beta,\end{aligned} \tag{2.24}$$

$$\Delta p_\lambda = \int_0^{2\pi}\frac{dp}{dx}\,dx, \tag{2.25}$$

$$F_\lambda = -\int_0^{2\pi} h^2\frac{dp}{dx}\,dx, \tag{2.26}$$

Were

$$\begin{aligned}
c_{11} &= \frac{a}{c\mu(1+\lambda_1)}, \qquad c_{22} = \frac{a^2\rho g}{c\mu}, \qquad c_3 = \frac{a^2\rho g\beta_1 T_0}{c\mu}, \qquad c_4 = \frac{a^2\rho g\beta_c c_0}{c\mu},\\
A &= \frac{1}{4M^2\eta\left(c_{11}\eta + M^2\cos^2\beta\right)}, \qquad m_{11} = \frac{K_T T_0\eta\,\csc\left(h\sqrt{\eta}\right)}{T_m c_0},\\
B &= \csc\left(h\sqrt{\eta}\right)\sec^2\beta\Big(-M^2m_{11}y + c_4M^2m_{11}y - 2c_{11}m_{11}y\eta + 2c_{11}c_4m_{11}y\eta\\
&\quad + c_{22}\eta(M^2 + 2c_{11}\eta)\cos(\alpha - h\sqrt{\eta}) - c_{22}M^2\eta\cos(\alpha + h\sqrt{\eta})\\
&\quad - 2c_{11}c_{22}\eta^2\cos(\alpha + h\sqrt{\eta}) + M^2m_{11}y\cos(2h\sqrt{\eta}) - c_4M^2m_{11}y\cos(2h\sqrt{\eta})\Big),\\
C &= 2c_{11}m_{11}y\eta\cos(2h\sqrt{\eta}) - 2c_{11}c_4m_{11}y\eta\cos(2h\sqrt{\eta}) + 2c_4M^2\eta\sin(h\sqrt{\eta})\\
&\quad - 2M^2\frac{dp}{dx}\eta\sin(h\sqrt{\eta}) + 4c_{11}c_4\eta^2\sin(h\sqrt{\eta}) - 4c_{11}\frac{dp}{dx}\eta^2\sin(h\sqrt{\eta})\\
&\quad + 2c_3M^2\eta\sin(y\sqrt{\eta}),\\
D &= M^2\cos(2\beta)\Big(-m_{11}y + c_4m_{11}y + c_{22}\eta\cos(\alpha - h\sqrt{\eta}) - c_{22}\eta\cos(\alpha + h\sqrt{\eta})\Big)\\
&\quad + m_{11}y\cos(2h\sqrt{\eta}) - c_4m_{11}y\cos(2h\sqrt{\eta}) + 2c_4\eta\sin(h\sqrt{\eta}) - 2\frac{dp}{dx}\eta\sin(h\sqrt{\eta})\\
&\quad + 2c_3\eta\sin(y\sqrt{\eta}).
\end{aligned} \tag{2.27}$$

The relationship between the velocity components (u, v) and the stream function Ψ is defined as

$$u = \frac{\partial\Psi}{\partial y}, \quad v = -\frac{\partial\Psi}{\partial x}. \tag{2.28}$$

From Eqs. (2.18) and (2.24), one can write

$$\Psi = \int u\,dy, \tag{2.29}$$

2.3. Particular case (Neglecting mass transfer):

Neglecting mass transfer in the medium, the above problem reduces to a peristaltic flow in symmetric channel with sinusoidal walls with heat transfer effect. By putting constants $c_4 = 0,\ K_T = 0,\ T_m = 0,$ in the field equations by incorporating this modification, the expressions of physical quantities can be deduced by adopting a similar approach, we get the peristaltic flow in symmetric channel with sinusoidal walls with heat transfer effect is obtained and the results agree with Elmhedy et al. [13].

2.4. Validity of the model

When the peristaltic flow (which is illustrated by mass transfer is ignored, peristaltic flow in symmetric channel with sinusoidal walls with heat transfer effect is obtained and the results agree with Elmhedy et al. [13].

In the present study, the viscous dissipation term in the heat conduction equation (2.5) is neglected. This simplification is justified by the parameter regime considered, where the contribution of viscous dissipation is expected to be small compared to other thermal effects. For studies where viscous dissipation is taken into account, see, for example[8].

3. Numerical Analysis and Discussion

The current section's goal is to carefully analyze the impact embedded parameters have on the flow quantities. The study done here is helpful for various parameter values. The peristaltic flow profile is examined under various parameters in the results section, along with an analysis of the profile's velocity, temperature, concentration, pressure gradient and pressure rise. The calculated results for different flow parameters in the studied problem are organized and presented using graphical depictions. These graphs offer a comprehensive and precise representation of the mathematical outcomes obtained in this study. Figures (2-6) illustrate the visual outcomes for temperature, velocity, pressure gradient, and pressure rise. Using the programming language MATHEMATICA, graphs are created to examine the impacts of the pertinent parameters listed above.

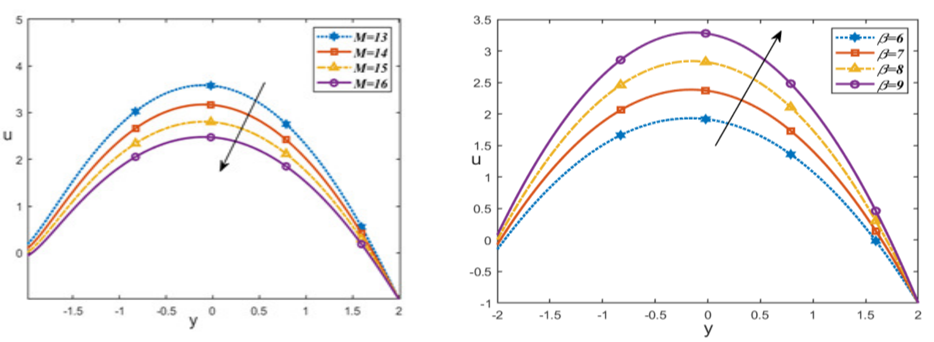

Figure 2: Variations of axial velocity u with respect to axial y for various values of β, M

Figure 2 shows the variations of velocity u with respect to y-axis for different values of Hartmann number M , and heat source /sink β respectively. It is observed that the velocity increases with increasing of β, while it decreases with increasing of M. In addition, it reaches its maximum at the center of the channel and its minimum at the channel's edges, satisfying the boundary conditions. Furthermore, the effect of the Hartmann number aligns with previous studies conducted by [5]. The complex characteristics of peristaltic flow are recognized for their ability to cause both simultaneous increases and drops, could be the cause of the fascinating phenomenon seen [30, 47].

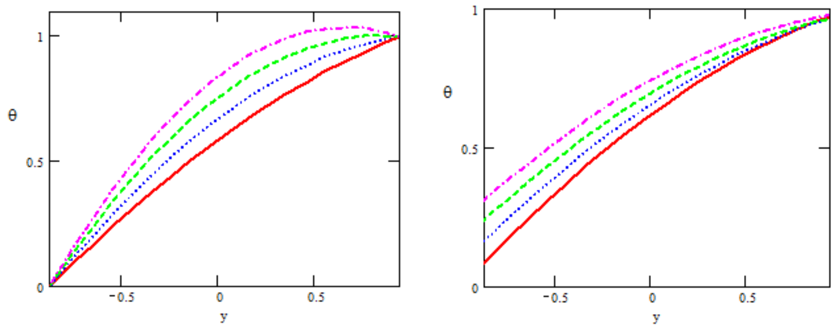

Figure 3: Variation of temperature θ with respect to axial coordinate y for different values of ε and k.

Figure 3 illustrates the variations of the temperature θ with respect to y-axis for different values of wave amplitude ε , and thermal conductivity k. It is noticed that the temperature increases with increasing of the parameter ε and k, respectively. In addition, it increases with an increase y-axis. The highest temperature occurs at the center of the channel, while the lowest appears at the edges. The temperature distribution also adheres to the specified boundary conditions. An important observation is that although the magnitudes of the horizontal and vertical particle motions vary slightly, the overall parabolic pattern remains constant. An important indication is as the peristaltic flow propagates across regions of varying channel depth, the amplitude of particle motion undergoes noticeable changes, leading to significant dynamic effects. This result is in a good agreement with the results obtained by Kalpana and Saleem [22].

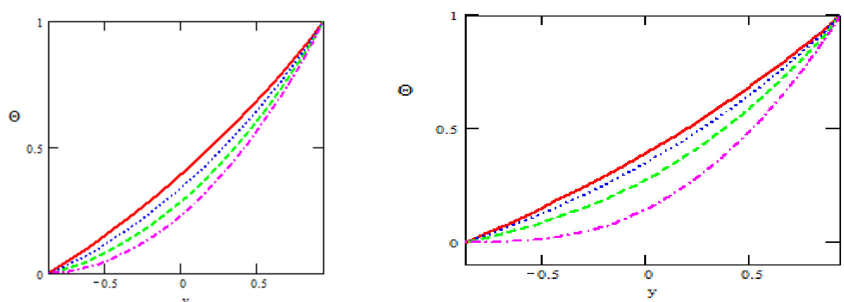

Figure 4: Variation of concentration φ with respect to axial coordinate y for different values of ε and k.

Figure 4 shows that the variations of concentration Θ with respect to y-axis for various values of the thermal conductivity k and the wave amplitude Ratio ε, respectively. It is observed that the concentration decreases with increasing of thermal conductivity k and the wave amplitude Ratio ε respectively, while it increases with increasing of y- axis. In Addition to, the concentration satisfied the boundary conditions. This resultis in a good agreement with the results obtained by Abdelhafez et al. [4].

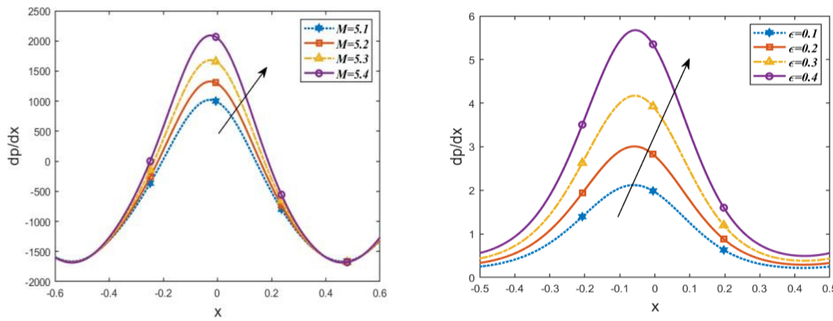

Figure 5: Variation of the pressure gradient $\frac{dp}{dx}$ with respect to axial x for different values of ε and M.

Figure 5 illustrates the behavior of the pressure gradient $\frac{\mathrm{dp}}{\mathrm{dx}}$ with respect to $x-$axis for different values of the parameters ϵ and M. It is noticed that the pressure gradient increases with increasing of M and ϵ respectively. In addition to, the pressure gradient exhibits oscillatory behavior along the entire $x-$range, highlighting how the pressure gradient $\frac{\mathrm{dp}}{\mathrm{dx}}$ changes relative to the axial x . The Hartmann number, which reflects the strength of the magnetic force, enables the fluid pressure to be regulated. This result is consistent with the findings of Ramesh and Divakar [31]. Since the pressure gradient controls the motion of fluid particles, it was observed from the results that the factors involved play a similar effect in the pressure gradient. This result is in a good agreement with the results obtained by Elshehawey et al. [14].

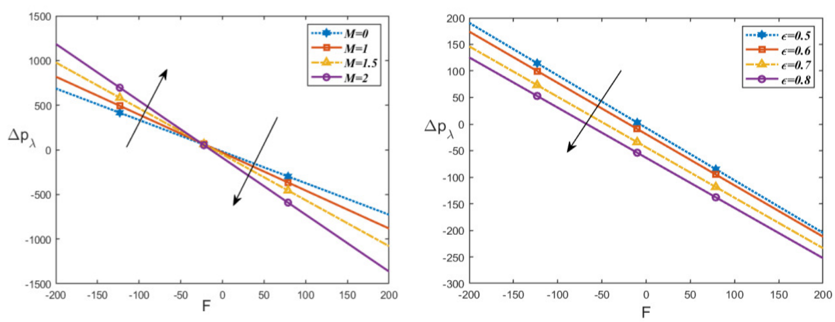

Figure 6: Variations of pressure rise ΔP_λ with respect to volume flow rate F for different values of ε, M.

Figure 6 illustrates the variations pressure rise Δp_λ with respect to volume flow rate F for different values of wave amplitude ratio , Hartmann number M, and Darcy number Da. It is observed that the pressure rise decreases with increasing of ϵ, while it increases with increasing of M within the range $-200 \leq$ F $\leq$ -25 and decline for -25 $\leq$ F $\leq$ 200. The channel peristalsis alone creates a free-pumping zone, while a pressure difference drives positive flow in the pumping region and assists flow in the co-pumping region via negative pressure difference. This result is in a good agreement with the results obtained by Abd-Alla et al. [1].

4. Conclusion

Recent studies have investigated the influence of heat transfer and magnetic fields on the peristaltic flow of Rabinowitsch fluid. These analyses consider fluid movement through a porous medium within an inclined channel. The key observations from these investigations are outlined below:

1. Axial velocity decreases with increasing Hartman number, but increases as the heat source/sink parameter β increases.

2. It has been noted that when the thermal conductivity k and the wave amplitude ratio ε grow, so does the temperature.

3. During peristalsis, this process results in a drop-in temperature. This suggests that temperature variations are influenced by the type of heat transfer occurring inside the system.

4. An increase in both the wave amplitude and thermal conductivity leads to a decrease in concentration.

5. As the aligned magnetic field and the wave amplitude ratio ε rise, the magnitude of $\frac{\mathrm{dp}}{\mathrm{dx}}$ increases.

6. It was noticed that the pressure gradient is affected by the magnetic field and the wave amplitude. As the Hartmann number increases, in the range from -200 to -25, the pressure gradient increases with the magnetic field. However, in the range from -25 to 200, the pressure gradient decreases as the Hartmann number increases. Also, when the wave amplitude increases, the pressure gradient decreases.

7. There are numerous uses for the current work in chemical engineering, which focuses on magnetohydrodynamic peristaltic flow.

8. There is a clear correlation between the parameter and the magnitude of the bolus. This demonstrates how changes in the fluid properties and channel geometry along the flow pattern influence the size of the bolus.

9. The results of this study may contribute to the development of digestive system pumping mechanisms and engineering systems. This analysis supports the smooth transport of body fluids, such as blood and lymph, through arteries and veins, which aids in oxygen delivery, waste removal, and other vital functions.

10. The outcomes of this study could benefit researchers working in science, medicine, engineering, and fluid mechanics. These results may serve as theoretical benchmarks for various parameters that influence peristaltic fluid flow, including the wave amplitude ε, the heat source/sink β, the Hartmann number, and the thermal conductivity k.

11. This fact helps in reducing temperature within various situations. Pressure gradient and heat transfer show oscillatory behavior. Concluding the study, we can say that peristaltic flow with consideration of ciliated walls enables us to cure various diseases related to respiratory. As Cilia are little brooms, sweeping mucus, bacteria, and dust particles out of our body down our neck and airways. We need these small sweepers to maintain smooth breathing. Infections can harm cilia, making them incapable of clearing allergens and dust from our airways.

Acknowledgement: The authors would like to acknowledge the Deanship of Graduate Studies and Scientific Research, Taif University, for funding this work.
Funding Statement: The author(s) received no specific funding for this study.

Author Contributions: Dr. Hanan S. Gafel: Her role in the research was as follows: she carried out the conceptualization of the study, developed the methodology, performed the validation, contributed to the investigation process, and supported the research through funding acquisition.

Mrs. Lolwah G. Albugami: Her role in the research was as follows: she carried out the formal analysis, prepared the original draft of the manuscript, and contributed to writing, reviewing, and editing the paper.

Supervision and Academic Guidance: Dr. S. Elhag and Dr. Mushrifah Al-Malki contributed through academic supervision, providing scientific guidance, critical review, and constructive feedback that enhanced the quality of the manuscript.

All authors reviewed the results and approved the final version of the manuscript

Conflicts of Interest: The authors declares no conflicts of interest to report regarding the present study.

References

1. Abd-Alla, A. M., Abo-Dahab, S. M., Abdelhafez, M. A., Elmhedy, Y., *Effect of heat and mass transfer on the nanofluid of peristaltic flow in a ciliated tube*, Scientific Reports 13, 16008, (2023).

2. Abd-Alla, A. M., Abo-Dahab, S. M., Thabet, E. N., Abdelhafez, M. A., *Heat and mass transfer for MHD peristaltic flow in a micropolar nanofluid: Mathematical model with thermophysical features*, Scientific Reports 12, 21540, (2022).

3. Abd-Alla, A. M., Abo-Dahab, S. M., Thabet, E. N., Abdelhafez, M. A., *Peristaltic pump with heat and mass transfer of a fractional second-grade fluid through a porous medium inside a tube*, Scientific Reports 12, 10608, (2022).

4. Abdelhafez, M. A., Abd-Alla, A. M., Abo-Dahab, S. M., Elmhedy, Y., *Influence of an inclined magnetic field and heat and mass transfer on the peristaltic flow of blood in an asymmetric channel*, Scientific Reports 13, 5749, (2023).

5. Adnan, F. A., Abdul Hadi, A. M., *Effect of an inclined magnetic field on peristaltic flow of Bingham plastic fluid in an inclined symmetric channel with slip condition*, Iraqi Journal of Science 60, 1551–1574, (2019).

6. Ali, H. A., *Radiative peristaltic transport of Ree–Eyring fluid through porous medium in asymmetric channel subjected to combined effect of inclined MHD and convective conditions*, International Journal of Physics: Conference Series 1879, 022101, (2021).

7. Ashraf, M. B., Rafiullah, Tanveer, A., Ulhaq, S., *Effects of Cattaneo–Christov heat flux on MHD Jeffery nanofluid flow past a stretching cylinder*, Journal of Magnetism and Magnetic Materials 565, 170154, (2023).

8. Baranovskii, E. S., *The stationary Navier–Stokes–Boussinesq system with a regularized dissipation function*, Mathematical Notes 115, 670–682, (2024).

9. Chandrawat, R. K., Joshi, V., Bég, O. A., Tripathi, D., *Computation of unsteady generalized Couette flow and heat transfer in immiscible dusty and non-dusty fluids with viscous heating and wall suction effects using a modified cubic B-spline differential quadrature method*, Heat Transfer 51, 99–139, (2021).

10. Choudhari, R., Tanveer, A., Ashraf, M. B., Ul-Haq, S., *Analysis of multiple slip effects on MHD blood peristaltic flow of Phan-Thien-Tanner nanofluid through an asymmetric channel*, International Journal of Modern Physics B 37, 2350102, (2023).

11. Das, S., Chakraborty, S., Sensharma, A., Jana, R. N., *Entropy generation analysis for magnetohydrodynamic peristaltic transport of copper–water nanofluid in a tube filled with porous medium*, Special Topics & Reviews in Porous Media: An International Journal 9, 217–228, (2018).

12. El-Dabe, N. T., Abou-Zeid, M. Y., Mohamed, M. A., Abd-Elmoneim, M. M., *MHD peristaltic flow of non-Newtonian power-law nanofluid through a non-Darcy porous medium inside a non-uniform inclined channel*, Archive of Applied Mechanics 91, 1067–1077, (2021).

13. Elmhedy, Y., Abd-Alla, A. M., Abo-Dahab, S. M., Alharbi, F. M., Abdelhafez, M. A., *Influence of inclined magnetic field and heat transfer on the peristaltic flow of Rabinowitsch fluid model in an inclined channel*, Scientific Reports 14, 4735, (2024).

14. Elshehawey, E. F., Eldabe, N. T., Elghazy, E. M., Ebaid, A., *Peristaltic transport in an asymmetric channel through a porous medium*, Applied Mathematics and Computation 182, 140–150, (2006).

15. Gafel, H. S., *Impact of magnetic field on a peristaltic flow with heat transfer of a fractional Maxwell fluid in a tube*, Computer Materials & Continua 72, 6141–6153, (2022).

16. Gafel, H. S., *Significance of heat transfer on the peristaltic pump of blood fluid under the inclined magnetic field*, Partial Differential Equations in Applied Mathematics, (2023).

17. Gafel, H. S., *The influence of magnetic fields and heat and mass transfer on peristaltic flow through a porous channel*, Journal of Computational and Theoretical Nanoscience 17, 4819–4825, (2020).

18. Hafez, N. M., Alsemiry, R. D., Alharbi, S. A., Abd-Alla, A. M., *Peristaltic transport characteristics of a second-grade dusty fluid with heat transfer through a tube revisited*, Scientific Reports 12, 1–23, (2022).

19. Hayat, T., Rafiq, M., Alsaedi, A., Ahmad, B., *Radiative and Joule heating effects on peristaltic transport of dusty fluid in a channel with wall properties*, European Physical Journal Plus 129, 1–7, (2014).

20. Iqbal, N., Yasmin, H., Bibi, A., Attiya, A. A., *Peristaltic motion of Maxwell fluid subject to convective heat and mass conditions*, Ain Shams Engineering Journal 12, 3121–3131, (2021).

21. Iqbal, N., Yasmin, H., Kometa, B. K., Attiya, A. A., *Effects of convection on Sisko fluid with peristalsis in an asymmetric channel*, Mathematical and Computational Applications 25, 52–60, (2020).

22. Kalpana, G., Saleem, S., *Heat transfer of magnetohydrodynamic stratified dusty fluid flow through an inclined irregular porous channel*, Nanomaterials 12, 1–13, (2022).

23. Khan, A. A., Tariq, H., *Peristaltic flow of second-grade dusty fluid through a porous medium in an asymmetric channel*, Journal of Porous Media 23, (2020).

24. Kothandapani, M., Srinivas, S., *On the influence of wall properties in the MHD peristaltic transport with heat transfer and porous medium*, Physics Letters A 372, 4586–4591, (2008).

25. Lakshminarayana, P., Sreenadh, S., Sucharitha, G., *The influence of slip, wall properties on the peristaltic transport of a conducting Bingham fluid with heat transfer*, Procedia Engineering 127, 1087–1094, (2015).

26. Makinde, O. D., Gnaneswara Reddy, M. M., *MHD peristaltic slip flow of Casson fluid and heat transfer in channel filled with a porous medium*, Scientia Iranica 26, 2342–2355, (2019).

27. Nunomura, S., Samsonov, D., Zhdanov, S., Morfill, G., *Heat transfer in a two-dimensional crystalline complex (dusty) plasma*, Physical Review Letters 95, 025003, (2005).

28. Palani, G., Ganesan, P., *Heat transfer effects on dusty gas flow past a semi-infinite inclined plate*, Forschung im Ingenieurwesen 71, 223–230, (2007).

29. Parthasarathy, S., Arunachalam, G., Vidhya, M., *Analysis on the effects of wall properties on MHD peristaltic flow of a dusty fluid through a porous medium*, International Journal of Pure and Applied Mathematics 102, 247–263, (2015).

30. Prasad, K. V., Vaidya, H., Rajashekha, C., Khan, S. U., Manjunatha, G., Viharika, J. U., *Slip flow of MHD Casson fluid in an inclined channel with variable transport properties*, Communications in Theoretical Physics 72, 095004, (2020).

31. Ramesh, K., Devakar, M., *Effect of heat transfer on the peristaltic transport of an MHD second grade fluid through a porous medium in an inclined asymmetric channel*, Chinese Journal of Physics 55, 825–844, (2017).

32. Reddy, Y. D., Ahmad, H., Tripathi, D., Prasad, K. V., *Heat absorption/generation effect on MHD heat transfer fluid flow along a stretching cylinder with a porous medium*, Alexandria Engineering Journal 64, 659–666, (2023).

33. Saffman, P. G., *On the stability of laminar flow of a dusty gas*, Journal of Fluid Mechanics 13, 120–128, (1962).

34. Selvi, C. K., Haseena, C., Srinivas, A. N., Sreenadh, S., *The effect of heat transfer on peristaltic flow of Jeffrey fluid in an inclined porous stratum*, IOP Conference Series: Materials Science and Engineering 263, 062027, (2017).

35. Sharma, T., Kumar, R., Vaidya, H., Raju, C. S. K., Vajravelu, K., *Numerical investigation of the hybrid ferrofluid flow in a heterogeneous porous channel with convectively heated and quadratically stretchable walls*, European Physical Journal Plus 138, 745, (2023).

36. Souayeh, B., Kumar, K. G., Mahabaleshwar, M. G., Rauf, A., *Slip flow and radiative heat transfer behavior of titanium alloy and ferromagnetic nanoparticles along with suspension of dusty fluid*, Journal of Molecular Liquids 290, 111223, (2019).

37. Srinivasacharya, D., Radhakrishnamacharya, G., Srinivasulu, C. H., *The effects of wall properties on peristaltic transport of a dusty fluid*, Turkish Journal of Engineering and Environmental Sciences 32, 357–365, (2009).

38. Tanveer, A., Ashraf, M. B., Masood, M., *Entropy analysis of peristaltic flow over a curved channel under the impact of MHD and convective conditions*, Numerical Heat Transfer, Part B: Fundamentals 85, 45–57, (2024).

39. Tanveer, A., Ashraf, M. B., Z-U-Nisa, *Analysis of entropy generation and Joule heating effects for MHD peristaltic flow over an asymmetric channel with mixed convective conditions*, Journal of Applied Mathematics and Mechanics 104, e202300089, (2024).

40. Tanveer, A., Ashraf, M. B., *Mixed convective flow of Sisko nanofluids over a curved surface with entropy generation and Joule heating*, Arabian Journal for Science and Engineering 48, 11263–11275, (2023).

41. Ul-Haq, S., Tanveer, A., Ashraf, M. B., Nawaz, R., *Artificial neural network (ANN) analysis of non-similar solution of MHD nanofluid flow past a curved stretching surface*, Numerical Heat Transfer: Applications, (2023).

42. Vaidya, H., Prasad, K. V., Tripathi, D., Choudhari, R., Hanumantha, H., Ahmad, H., *Viscoplastic hybrid nanofluids flow through vertical stenosed artery*, BioNanoScience 13, 2348–2370, (2023).

43. Vaidya, H., Rajashekhar, C., Manjunatha, G., Prasad, K. V., *Effect of variable liquid properties on peristaltic flow of a Rabinowitsch fluid in an inclined convective porous channel*, European Physical Journal Plus 134, 231, (2019).

44. Vaidya, H., Tripathi, D., Mebarek-Oudina, F., Rajashekhar, C., Baskonus, H. M., Prasad, K. V., Shivaleela, *Scrutiny of MHD impact on Carreau–Yasuda (CY) fluid flow over a heated wall of the uniform micro-channel*, Chinese Journal of Physics 87, 766–781, (2024).

45. Vajravelu, K., Sreenadh, S., Lakshminarayana, P., *The influence of heat transfer on peristaltic transport of a Jeffrey fluid in a vertical porous stratum*, Communications in Nonlinear Science and Numerical Simulation 16, 3107–3125, (2011).

46. Zeeshan, A., Ijaz, N., Bhatti, M. M., Mann, A. B., *Mathematical study of peristaltic propulsion of solid-liquid multiphase flow with a biorheological fluid as the base fluid in a duct*, Chinese Journal of Physics 55, 1596–1604, (2017).

47. Zhang, L., Bhatti, M. M., Michaelides, E. E., *Thermally developed coupled stress particle-fluid motion with mass transfer and peristalsis*, Journal of Thermal Analysis and Calorimetry 143, 2515–2524, (2021).

Hanan S. Gafel,
Department of Mathematics and Statistics,
College of Science, Taif University,
P.O. Box 11099, Taif 21944, Saudi Arabia
E-mail address: h.gafal@tu.edu.sa

and

Luluah G. Albugami,
Department of Mathematics and Statistics,
College of Science, Taif University,
P.O. Box 11099, Taif 21944, Saudi Arabia
E-mail address: s44580268@students.tu.edu.sa

and

S. H. Elhag,
Department of Mathematics and Statistics,
College of Science, Taif University,
P.O. Box 11099, Taif 21944, Saudi Arabia
E-mail address: h.sfaa@tu.edu.sa

and

Mushrifah. A. S. Al-Malki,
Department of Mathematics and Statistics,
College of Science, Taif University,
P.O. Box 11099, Taif 21944, Saudi Arabia
E-mail address: m.malky@tu.edu.sa